# Improved Supercapacitor Performance of $MnO_2$-Electrospun Carbon Nanofibers Electrodes by mT Magnetic Field

By: Zheng Zeng, Yiyang Liu, Wendi Zhang, Harish Chevva, and Jianjun Wei

Z. Zeng, Y. Liu, W. Zhang, H. Chevva, J. Wei, Improved Supercapacitor Performance of $MnO_2$-Electrospun Carbon Nanofibers Electrodes by mT Magnetic Field, *Journal of Power Sources*, **2017**, 358, 22-28. https://doi.org/10.1016/j.jpowsour.2017.05.008



## Abstract:

This work reports on a finding of mT magnetic field induced energy storage enhancement of $MnO_2$-based supercapacitance electrodes (magneto-supercapacitor). Electrodes with $MnO_2$ electrochemically deposited at electrospun carbon nanofibers (ECNFs) film are studied by cyclic voltammetry (CV), galvanostatic charge/discharge, electrochemical impedance spectroscopy (EIS), and life cycle stability tests in the presence/absence of milli-Tesla (mT) magnetic fields derived by Helmholtz coils. In the presence of a 1.34 mT magnetic field, $MnO_2$/ECNFs shows a magneto-enhanced capacitance of 141.7 F $g^{-1}$ vs. 119.2 F $g^{-1}$ (~19% increase) with absence of magnetic field at a voltage sweeping rate of 5 mV $s^{-1}$. The mechanism of the magneto-supercapacitance is discussed and found that the magnetic susceptibility of the $MnO_2$ significantly improves the electron transfer of a pseudo-redox reaction of Mn(IV)/Mn(III) at the electrode, along with the magnetic field induced impedance effect, which may greatly enhance the interface charge density, facilitate electrolyte transportation, and improve the efficiency of cation intercalation/de-intercalation of the pseudocapacitor under mT-magnetic field exposure, resulting in enhancement of energy storage capacitance and longer charge/discharge time of the $MnO_2$/ECNFs electrode without sacrificing its life cycle stability.

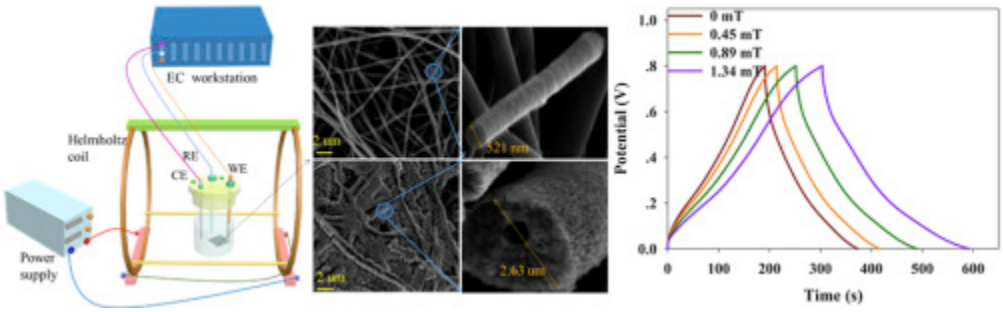


**Keywords:** Manganese dioxide | Pseudocapacitor | Carbon nanofibers | Magnetic field | Energy storage enhancement

**Article:**

## 1. Introduction

Electrochemical double layer supercapacitors have drawn a lot of attention due to fast charging/discharging rate, increased energy density and power density, and large life cycle stability [1], [2], [3], [4]. However, regarding the energy storage capability, there is an emerging need to develop supercapacitors with high relative dielectric constant or redox reactions in the double layer and surface area of the electrode for higher energy density and larger life cycle stability [5], [6], [7]. Some of the electroactive metal oxides, e.g. ruthenium oxide ($RuO_2$) [8], manganese oxide ($MnO_x$) [9], nickel oxide ($NiO_x$) [10], cobalt oxide ($Co_3O_4$) [11], tin oxide ($SnO_2$) [12], zinc oxide (ZnO) [13], and vanadium (V) oxide ($V_2O_5$) [14] etc. were used in supercapacitor (so-called pseudocapacitor) electrodes to offer fast and reversible redox reactions, contributing to higher energy density capacity [15]. To increase surface area, carbon nanomaterials, such as carbon nanotubes (CNTs) [16], carbon nanofibers (CNFs) [17], graphene nanofoam (GF) [18], and reduced graphene oxide (rGO) [19] were used in supercapacitors, which not only provide unique size and surface dependent properties but also excellent intrinsic physical (e.g. electrical, thermal, chemical and mechanical) properties. Among these, electrospun carbon nanofibers (ECNFs) is known for its large porosity, high conductivity, low cost in production with freestanding nature, and good scaffolds to uniformly support nanostructured metal oxide [20]. Electrospinning is an efficient fiber production method which uses electric force to draw charged threads of polymer solutions or polymer melts up to form polymer nanofibers [21] which can be converted to porous ECNFs with subsequent carbonization [22]. Electrospinning has become a powerful and easy method to form carbon nanofibers in large scale for broad applications. It has been used for electrode material production or separator materials for supercapacitors [23], [24], [25], Li (or Na)-ion batteries [26], [27], [28], [29], and preparation of electrical double-layer capacitor half-cells [30].

Recently, the influence of an external magnetic field over the capacitance of electrodes has won some attention due to effects of Lorentz force acting on moving charges/ions, charge density gradient modulation, electron state excitation and oscillatory magnetization [31], [32], [33], thus energy storage improvement. Two strategies of using magnetic field for enhancing the electrochemical process in capacitors have been demonstrated. One is to introduce magnetic nanoparticles into the electrode in the presence of an external magnetic field. For instance, $Fe_2O_3$/graphene nanocomposites [33], $Fe_3O_4$/active carbon nanocomposites [34], and $Fe_3O_4$/active carbon nanocomposites [35] demonstrated enhancement of the capacitance and energy density with an external magnetic field. The other one is to reconstruct the charge density and electric polarization in the magnetic material system. For example, ionic liquid was used in charge carrier engineering to achieve tunable dielectric permittivity [31].

During the past years, $MnO_2$ has been one of the most commonly used transition-metal oxides that have been used as pseudocapacitive electrode materials due to its unique characteristics, such as easy-for-deposition, stability and significantly enhanced energy storage performance [36], [37]; however, little is known about the magnetic field effect on its energy storage. Herein, for the first time, we present a magnetization-induced capacitance enhancement in $MnO_2$/ECNFs nanocomposite electrodes fabricated by electrochemical deposition of $MnO_2$ on

ECNFs. The $MnO_2$/ECNFs electrode was characterized by scanning electron microscopy (SEM), x-ray powder diffraction (XRD), energy-dispersive x-ray spectroscopy (EDX), Raman spectroscopy, Fourier transform infrared spectroscopy (FTIR), thermogravimetric analysis (TGA), and superconducting quantum interference device vibrating sample magnetometer (SQUID VSM). The electrochemical performance of the $MnO_2$/ECNFs electrodes for capacitive energy storage was studied by cyclic voltammetry (CV), galvanostatic charge/discharge, electrochemical impedance spectroscopy (EIS), and life cycle stability tests in the presence/absence of milli-Tesla (mT) to sub-mT magnetic fields derived by Helmholtz coils.

## 2. Results and discussion

The morphologies of ECNFs and $MnO_2$/ECNFs were characterized by SEM (Fig. 1b,d). The ECNFs with nanofiber diameter of about 521 nm (Fig. 1c) are decorated by $MnO_2$ coating with thickness of ~2.1 μm making a total diameter of the fiber as about 2.63 μm (Fig. 1e). The charge current of 40 μA, the charge time of 3 h in an aqueous precursor solution containing 10 mM $MnSO_4$ and 100 mM $Na_2SO_4$ were applied to achieve the electrochemical deposition of the $MnO_2$ at the 1 $cm^2$ ECNFs film. The success of $MnO_2$ deposition was confirmed with Raman spectra (Fig. S1 Mn—O at the Raman shift of 627 $cm^{-1}$), XRD pattern (in Fig. S2, the well resolved peak at 37.1° is attributed to $MnO_2$), and FTIR spectra (in Fig. S3, Mn—O stretch is presented at the wavenumber of 648 $cm^{-1}$ and 731 $cm^{-1}$) [38], [39]. TGA shows the weight fraction of $MnO_2$ in the $MnO_2$/ECNFs electrode is about 53% (Fig. S4), which was further verified using EDX analysis by averaging different spectrum zones (Fig. S5).

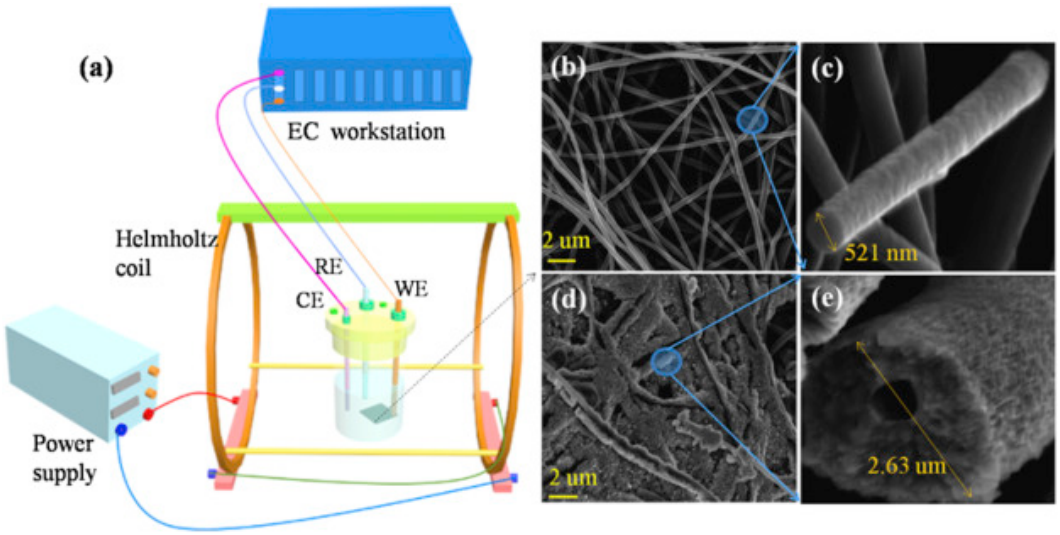


**Fig. 1.** (a) The schematic illustration of the electrochemical cell setup in the presence of an external magnetic field. (b)–(e) SEM images of the electrode materials (b) ECNFs, (c) enlarged ECNFs, (d) $MnO_2$/ECNFs, and (e) enlarged $MnO_2$.

As a pseudocapacitive electrode, the $MnO_2$/ECNFs electrode possesses combined contribution of spacers and redox reaction, i.e., the electrochemical double layer capacitance and the pseudocapacitance from $MnO_2$ for energy storage. The former stores charge electrostatically due to the adsorption of ions at electrode surfaces and is mainly determined by the electrode surface area. While, for the latter, the energy is stored in virtue of highly reversible redox reactions

(e.g. electron transfer reactions) between Mn(IV)/Mn(III) species and cation intercalation/de-intercalation at the $MnO_2$/electrolyte interfaces [36], [40], [41]. The charge storage mechanism of the $MnO_2$/ECNFs electrode involving the KOH electrolyte can be expressed as [36], [42]:

$$Mn(IV)O2 + mH^+ + nK^+ \leftrightarrow Mn(III)Mn(IV)OOH_mK_n \quad (1)$$

Equation (1) represents the successive multiple surface redox reactions between the Mn(IV)/Mn(III) complexes leading to the pseudo-capacitive charge storage mechanism [42].

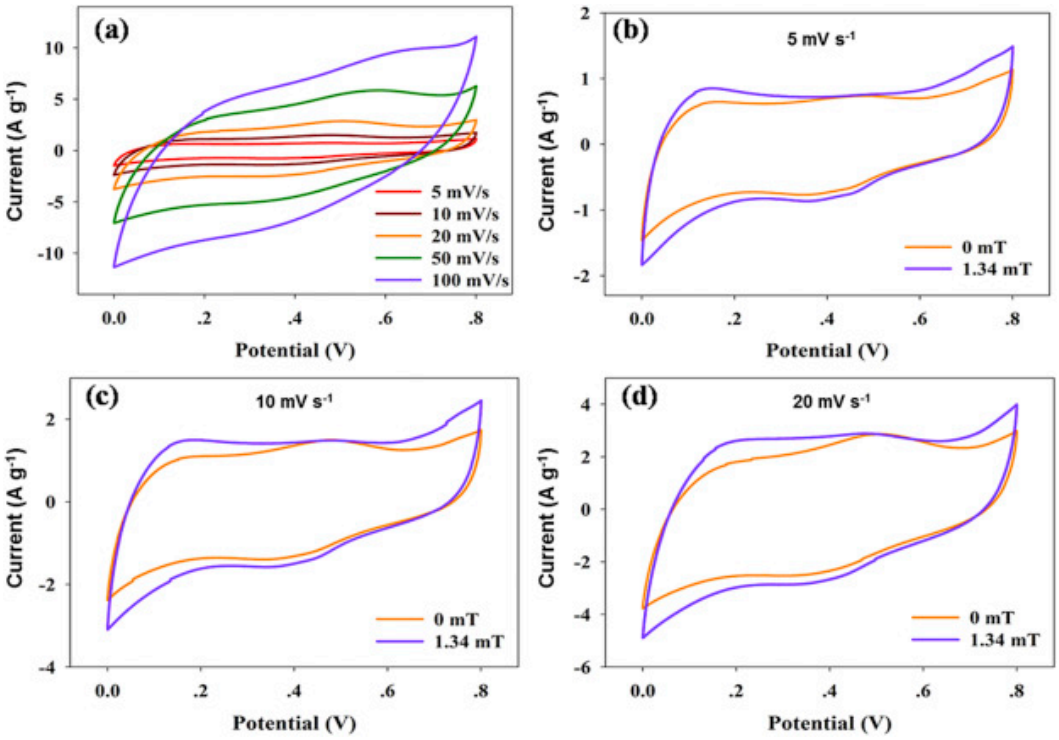


**Fig. 2.** (a) Cyclic voltammetry loops of the $MnO_2$/ECNFs electrodes tested in the absence of magnetic field (0 mT) at different voltage sweeping rates. Cyclic voltammetry loops of the $MnO_2$/ECNFs electrodes tested in the presence (1.34 mT)/absence (0 mT) of magnetic field at different scan rates of 5 mV $s^{-1}$ (b), 10 mV $s^{-1}$ (c), 20 mV $s^{-1}$ (d).

To measure the specific capacitance of the $MnO_2$/ECNFs electrode and magnetic field effect, CV was performed using the classical three-electrode method [43] in a 6.0 M KOH electrolyte solution. Fig. 2 shows the representative, stable cyclic voltammetry (CV) loops with or without an external magnetic field, which present a combination of both double layer and pseudocapacitive behaviors within the scan voltage from 0.0 V to 0.8 V. There are a pair of peaks at the voltage between 0.4 and 0.5 V vs. Ag/AgCl which might be attributed to the redox reaction of the Mn(IV)/Mn(III) species in the form of $K^+$ intercalation [41]. The overall specific capacitance is calculated from the integrated area of the CV loops (see details in Supplementary information, SI). In the absence of an external magnetic field, the specific capacitance of the $MnO_2$/ECNFs electrode was calculated to be 119.2, 105.8, 92.8, 71.0, 53.4 F $g^{-1}$ at the voltage sweeping rates of 5, 10, 20, 50, and 100 mV $s^{-1}$, respectively. Compared to that of the ECNFs-only electrode (Fig. S6a), $MnO_2$/ECNFs shows higher capacitance because of the higher relative dielectric constant of $MnO_2$ and its pseudo-activity. In the presence of 1.34 mT magnetic field,

the capacitance of the $MnO_2$/ECNFs magneto-supercapacitor electrode was obtained to be 141.7, 125.9, 110.2, 86.5, 67.0 $Fg^{-1}$ at the same voltage sweeping rates of 5, 10, 20, 50, and 100 mV $s^{-1}$, respectively, which increased by about avg. 19% for all sweeping rates (Fig. 2b–d, Fig. S7). Since there is no measurable enhancement of capacitance of the ECNFs-only electrodes at the same range of voltage sweeping rates (Fig. S6) under the magnetic field, one can conclude that the magnetocapacitance enhancement of the $MnO_2$/ECNFs electrode is resultant from the magnetic field effect on the $MnO_2$ at the ECNFs substrate.

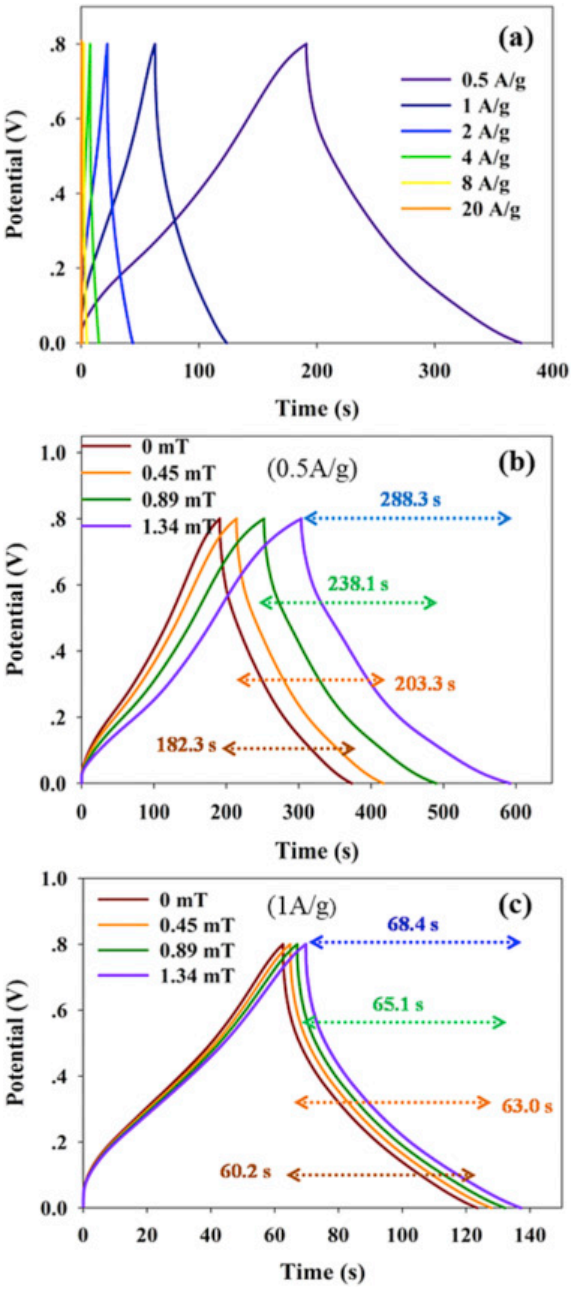


**Fig. 3.** (a) Galvanostatic charge/discharge curves of the $MnO_2$/ECNFs electrodes tested in the absence of magnetic field under different current densities. Galvanostatic charge/discharge curves of the $MnO_2$/ECNFs tested in the presence of different magnetic fields under different current densities of 0.5 A $g^{-1}$ (b), and 1 A $g^{-1}$ (c).

The effect of magnetization on the galvanostatic charge/discharge performance of $MnO_2$/ECNFs was studied under different current densities (0.5–20 A $g^{-1}$, Fig. 3abc & Fig. S8). The curvature of the charge step between the voltage of 0.0–0.4 V and larger growth of the discharge curve between the same range voltages suggest a combined contribution from pseudocapacitance and double layer capacitance [44], which is consistent with the observation from the CV studies. With the applied magnetic field from 0.45 mT to 1.34 mT and the same current density, the charge/discharge time increases (Fig. 3 b–c, Fig. S8) comparing to that of the absence of magnetic field. The charge/discharge time under smaller current density increases more significantly than that of the larger current density (e.g. 58.1% increase at 0.5 A $g^{-1}$ vs. 13.6% at 1 A $g^{-1}$ with 1.34 mT magnetic field), suggesting the magnetic field effects on both the pseudocapacitive electrolyte-electrode interface and double layer region, resulting in the magneto-capacitance enhancement.

From the charge/discharge curves, specific capacitance is calculated from the discharge curves [45], i.e., $C = I \cdot t/(m \cdot \Delta E)$, in which $I$ is the discharge current, $t$ is the discharge time, and $\Delta E$ is the potential drop during discharge in V (see more in SI). It was found that, under the magnetic field of 1.34 mT, the electrode of $MnO_2$/ECNFs enhanced the capacitance by 58.1% (Fig. 3b) at the current density of 0.5 A $g^{-1}$, by 13.6% at 1 A $g^{-1}$ (Fig. 3c) and 6% at 2 A $g^{-1}$ (Fig. S8), respectively. Moreover, to quantitatively analyze the pseudocapacitance contribution to the overall capacitance performance, the non-faradaic contribution from double layer capacitance and the faradaic contribution from pseudocapacitance were separated in galvanostatic charge-discharge curves [44], [46]. By considering the area corresponding to faradaic contribution in $MnO_2$/ECNFs electrode, at current density of 0.5 A $g^{-1}$, the pseudocapacitance contribution from $MnO_2$ in overall performance was approximately 56.5%, 61.0%, 62.4%, and 67.8% with the applied magnetic field of 0 mT, 0.45 mT, 0.89 mT, and 1.34 mT, respectively. The fraction of the pseudocapacitive contribution in energy storage increases along with the magnetic field strength, suggesting the more significant effect on the pseudo-redox reaction by the magnetic field at the $MnO_2$/ECNFs electrode than that on the non-faradaic contribution.

Next, the effect of magnetic field on the impedance of the $MnO_2$/ECNFs within the electrochemical cell (6 M KOH electrolyte) was investigated using EIS, which may provide understanding of the different electrochemical behaviors in the absence/presence of magnetic field. Fig. 4 shows the performance of EIS for the $MnO_2$/ECNFs electrodes by setting the working electrode voltage at 0.0 V vs. Ag/AgCl over the frequency range of 10 kHz to 0.01 Hz with the potential amplitude of 10 mV. Both the Nyquist plots of EIS spectra in the absence/presence of an external magnetic field show a semicircle arc in the high frequency region and a linear line in the low frequency region, indicating a low internal resistance of the $MnO_2$/ECNFs electrodes [47]. In the presence of 1.34 mT magnetic field, the capacitor system superficially seems to be a more ideal double layer supercapacitor, since the semicircle arc is more obvious and straight line seems to be little more vertical. Zhu et al. [33], [47] reported that additional Lorentz force acts on the moving ions in a perpendicular magnetic field flux density (magnetohydrodynamic phenomenon), which may promote the electrolyte convection in the bulk electrolyte. Hence, it is not surprising that the changes of the solution resistance ($R_s$ ~1 Ohms) in bulky electrolyte, the charge transfer resistance ($R_{ct}$) at the electrode-electrolyte interface, and

the leakage resistance ($R_{leak}$) of the double layer region at low frequency are observed for $MnO_2$/ECNFs electrodes under magnetic field. Specifically, the solution resistance (Rs) with 1.34 mT magnetic field decreases about 0.1 Ohms from 1 Ohms. The resistance of charge transfer ($R_{ct}$) of the electrode reaction obtained from the diameter of the semicircle in the high frequency region (1.26 Ohms) decreased from 1.35 Ohms of the non-magnetized $MnO_2$/ECNFs electrode, indicating a faster contact and charge transfer which may result in an improved rate performance [48]. The low frequency leakage resistance ($R_{leak}$) [34] in the double layer region increased for the $MnO_2$/ECNFs electrode with the presence of magnetic field, suggesting that leakage current flowing across the double layer at the electrode-electrolyte interface was better restricted, which may also improve the $MnO_2$/ECNFs electrode capacitance.

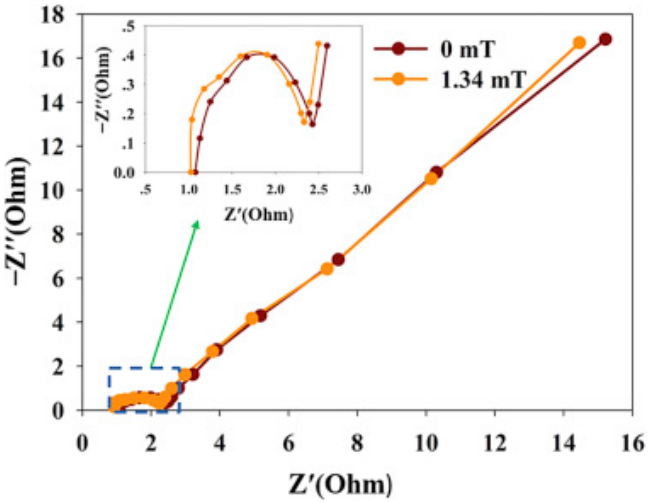


**Fig. 4.** Nyquist plots of the $MnO_2$/ECNFs electrodes tested in the presence (1.34 mT)/absence (0 mT) of magnetic field.

The EIS analysis of this work agrees with the previous studies by Zhu et al. [33], [47] on different metal oxide (Fe, Ni, Co)-carbon supercapacitors. The magnetohydrodynamic phenomenon is the major factor for the electrode internal resistance decrease and the magnetic induced electrolyte convection to reach extra electrode surfaces, which may help to generate larger specific capacitance of the electrodes, and build up a complete double layer that restricts the leakage of free electrons, thus improving the capacitance performance. However, in this study, much smaller magnetic field strength, i.e. 1.34 mT on $MnO_2$/ECNFs electrode and much smaller resistance change, achieved comparable capacitance enhancement of 72 mT magnetic field on metal-oxide (Fe, Ni, Co) nanocomposite electrodes [33], [47]. It is known that $MnO_2$ has the paramagnetic property due to multiple unpaired electrons involving in the pseudo-active electron transfer reaction. Hence it may help to better understand the capacitance enhancement by measuring the magnetization of the $MnO_2$/ECNFs electrodes.

The magnetic susceptibility of the $MnO_2$/ECNFs was performed using the SQUID VSM at room temperature and Fig. 5 shows the moment response of the $MnO_2$/ECNFs electrode under different magnetic field strength. The magnetization, measured as the magnetic moment associated with electron's spin state, $\mu_e$, at 1.34 mT magnetic field is found to be $4.23 \times 10^{-4}$ emu $g^{-1}$ of the $MnO_2$/ECNFs electrode and $\sim 7.98 \times 10^{-4}$ emu $g^{-1}$ with respect to the pure $MnO_2$ mass fraction (ca. 53%) in the electrode. The spin-dependent torque the $MnO_2$ experienced,

representing the improved energy state of the electron, is $1.07 \times 10^{-9}$ J $g^{-1}$ ($\sim 93.0 \times 10^{-9}$ J $mol^{-1}$) obtained from multiplying the magnetic field by the magnetic moment. The magnetic field induced spin-dependent torque on an electron with spin quantum number $m_s = +1/2$ and $-1/2$ causes the degeneracy, namely different energy levels of the "+" and "−" spin states [49]. which is expressed as, $h\nu = g\beta H$ where $h\nu$ is the quantum of energy corresponding to a characteristic frequency $\nu$, $g$ is dimensionless constant called the "electron g-factor", $\beta$ is the electronic Bohr magneton ($9.2740154 \times 10^{-24}$ J $T^{-1}$), and $H$ is the magnetic field strength. The enhanced energy state of the electrons increases the electron transfer kinetics between the species of Mn(IV)/Mn(III), as well as the electron transportation efficiency at the electrolyte-$MnO_2$/ECNTs interfaces, hence contributes to the capacitance enhancement.

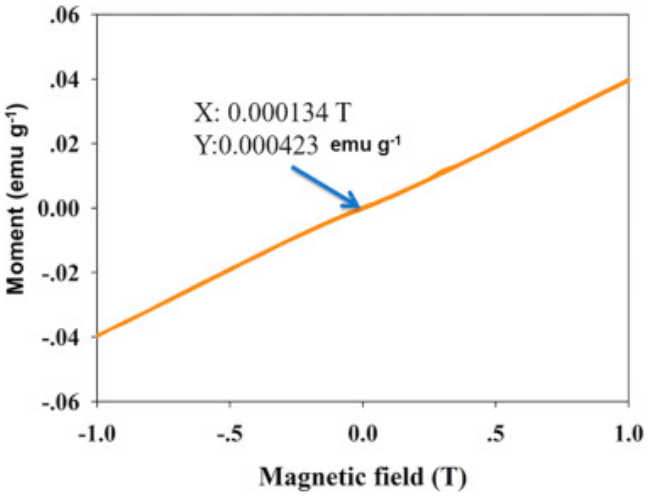


**Fig. 5.** SQUID VSM result of $MnO_2$/ECNFs at room temperature. The closely straight line shows the magnetization of $MnO_2$/ECNFs is $4.23 \times 10^{-4}$ emu $g^{-1}$ at 1.34 mT magnetic field. Since the weight ratio of $MnO_2$ in $MnO_2$/ECNFs is about 53%, the magnetization on pure $MnO_2$ is calculated to be $7.98 \times 10^{-4}$ emu $g^{-1}$.

The magnetic field effect on the redox electron transfer kinetics of Mn(IV)/Mn(III) is further analyzed according to the classical transition state theory by considering the contribution of the enhanced electron energy states to the activation energy due to magnetic field induced degeneracy. The rise of Zeeman energy, $g\beta HS$ ($S$ is spin), relative to the reactant energy when there is no applied field, of the unpaired electrons in $MnO_2$ with magnetic field contributes to the activation energy by reducing the net enthalpy of activation barrier and thus the reaction rate is facilitated. The redox electron transfer rate of Mn(IV)/Mn(III) at the electrode can be expressed in an Arrhenius form as (see details in SI):

$$k_m = A \exp\left[\frac{\Delta S_0^*}{k_b}\right] \exp\left[\frac{\Delta S_m^*}{k_b}\right] \exp\left[-\frac{\Delta H_0^*}{k_b T}\right] \exp\left[-\frac{\Delta H_m^*}{k_b T}\right] \quad (2)$$

with $\Delta H_m^* = -gHS\beta$, A is the pre-factor depending on the convolution of a suitable weighted frequency ($\nu_n$) for crossing the activation barrier and the transmission coefficient or averaged transition probability for electron transfer per passage of the system through the intersection region from reactant to product, and in classical transition theory, A is taken as $k_b T/h$ where $k_b$ is Boltzmann's constant, T is absolute temperature, and $h$ is Planck constant.

With sufficient magnetic field for the energy degeneracy of single unpaired electron spin, the electron transfer rate can be doubled (see SI). The measured magnetic susceptibility response to the external magnetic field suggests that the $MnO_2$/ECNTs electrode is sensitive to magnetic field due to the multiple unpaired electron spins of $MnO_2$. While it is difficult to quantitatively analyze how the field impact the electron transfer in the electrode, these analyses suggest that the facilitated electron transfer kinetics of the pseudo-redox reaction in the $MnO_2$/ECNFs electrode contributes significantly in the energy storage performance with respect to the small magnetic field applied to the electrode.

Based on these results and analyses, one can find that the mT magnetic field significantly enhances energy storage capacitance of the $MnO_2$/ECNFs electrodes with a comprehensive mechanism due to the combined contribution of both the double layer and pseudo-active capacitance. Firstly, the change of the electrode resistance in electrochemical cell, though small, suggests that the change of dipole moment in the transition and vibrational states of electrolyte at the double layer area can improve the conductivity and reduce the resistance (impedance effect), thus enhance the electrochemical adsorption/desorption of cations and anions at the electrode/electrolyte interfaces; Secondly, and more significantly in this case, the paramagnetic nature of the $MnO_2$ with multiple unpaired electrons and magnetic susceptibility may largely facilitate the Mn(IV)/Mn(III) pseudo-redox reaction and electron transfer to the electrolyte-electrode interfaces, which may result in higher charge density at the electrode interfaces, more efficiency of cation intercalation/de-intercalation, and thicker double layer, therefore the enhanced capacitance. Since both the impedance effect and the electron spin energy degeneracy depend on the strength of the magnetic field, the dissimilarity of the magneto-capacitance enhancement at different magnetic field during charge and discharge process is expected.

Finally, for practical purpose, the life cycle performance of the $MnO_2$/ECNFs electrodes was performed by galvanostatic charge/discharge cycling in term of two important parts, i.e., cycling capability or capacitance retention, and total discharge time. As shown in Fig. 6, in the absence of 1.34 mT magnetic field, 92.3% of the initial capacitance was maintained after 1000 cycles. With presence of 1.34 mT magnetic field, 90.6% of the initial capacitance was maintained after 1000 cycles. Note that with the same number of cycling, the total discharge time increased by 15.1% with presence of magnetic field (Fig. 6 inserted) due to magnetic field induced discharge time extension. Experimental performance and data analysis indicate that the magnetic susceptibility largely increases the charge transfer rate thus improves the pseudo-reactions of $MnO_2$ at the electrode and interfaces. A supercapacitor nanocomposite electrode composed of $MnO_2$ deposition on ECNFs exhibits significantly enhanced galvanostatic charge/discharge cycling at a 1.34 mT of magnetic field even under a high current density of 4 A $g^{-1}$, suggesting that the enhanced magneto-supercapacitive performance is mainly attributed to magnetic susceptibility of the $MnO_2$ in the electrode because of the improvement of the pseudocapacitive behavior at the electrode and the electrode/electrolyte interfaces.

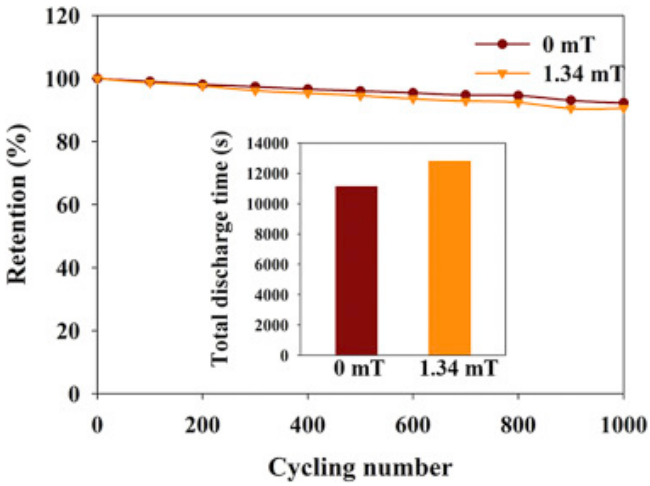


**Fig. 6.** Cycling performance of the $MnO_2$/ECNFs electrodes tested in the presence (1.34 mT)/absence (0 mT) of magnetic field under the current density of 4 A $g^{-1}$.

## 3. Conclusion

In summary, after applying a 1.34 mT magnetic field, $MnO_2$/ECNFs showed enhanced magneto-capacitance of 141.7 F $g^{-1}$ at the cyclic voltage sweeping rates of 5 mV $s^{-1}$. The capacitance of $MnO_2$/ECNFs was increased by 58.1% at the current density of 0.5 A $g^{-1}$ during the galvanostatic charge/discharge test. Meanwhile, in the presence of 1.34 mT magnetic field, the magneto-supercapacitor presented "low resistance shift" for bulk electrolyte and the $MnO_2$/ECNFs electrode. Longer charge/discharge time of the electrode is observed under magnetic field than that without magnetic field, while did not sacrifice its life cycle stability. The insightful discussion of the potential mechanism suggests that the magneto-supercapacitance enhancement can be primarily attributed to the magnetic susceptibility of $MnO_2$ induced electron spin energy degeneracy for facilitated electron transfer reaction, the magnetohydrodynamic impact on electrolyte transportation and improved cation intercalation/de-intercalation under the mT magnetic field, thus resulting in higher charge density at the electrode/electrolyte interfaces, thicker double layer, and lower internal resistance. This study may pave a way to the development of sustainable metal oxide-based supercapacitors with magneto-capacitance enhancement by applying a low magnetic field.

## Acknowledgement

This work is supported by NC state fund through Joint School of Nanoscience and Nanoengineering (JSNN). The authors would like to thank Dr. Lifeng Zhang at North Carolina A&T State University for helping on ECNF fabrication, Dr. Lewis Reynolds and Dr. Raj Kumar in North Carolina State University for the SQUID VSM test, and Dr. Rui Li in North Carolina A&T State University for the TGA test. This work was performed at the JSNN, a member of Southeastern Nanotechnology Infrastructure Corridor (SENIC) and National Nanotechnology Coordinated Infrastructure (NNCI), which is supported by the National Science Foundation (ECCS-1542174).

## Appendix A. Supplementary data

Supplementary data related to this article can be found at http://dx.doi.org/10.1016/j.jpowsour.2017.05.008.

**References**


[1] N.-S. Choi, Z. Chen, S.A. Freunberger, X. Ji, Y.-K. Sun, K. Amine, G. Yushin, L.F. Nazar, J. Cho, P.G. Bruce, Angew. Chem. Int. Ed. 51 (2012) 9994e10024.

[2] J.R. Miller, R.A. Outlaw, B.C. Holloway, Science 329 (2010) 1637.

[3] H. Itoi, H. Nishihara, T. Kogure, T. Kyotani, J. Am. Chem. Soc. 133 (2011) 1165e1167.

[4] G. Yu, L. Hu, M. Vosgueritchian, H. Wang, X. Xie, J.R. McDonough, X. Cui, Y. Cui, Z. Bao, Nano Lett. 11 (2011) 2905e2911.

[5] S.-E. Chun, B. Evanko, X. Wang, D. Vonlanthen, X. Ji, G.D. Stucky, S.W. Boettcher, Nat. Commun. 6 (2015) 7818.

[6] H.-J. Choi, S.-M. Jung, J.-M. Seo, D.W. Chang, L. Dai, J.-B. Baek, Nano Energy 1 (2012) 534e551.

[7] C. Lian, K. Liu, K.L. Van Aken, Y. Gogotsi, D.J. Wesolowski, H.L. Liu, D.E. Jiang, J.Z. Wu, ACS Energy Lett. 1 (2016) 21e26.

[8] W. Wang, S. Guo, I. Lee, K. Ahmed, J. Zhong, Z. Favors, F. Zaera, M. Ozkan, C.S. Ozkan, Sci. Rep. 4 (2014) 4452.

[9] Y. Jiang, X. Ling, Z. Jiao, L. Li, Q. Ma, M. Wu, Y. Chu, B. Zhao, Electrochim. Acta 153 (2015) 246e253.

[10] Y. Jiang, P. Wang, X. Zang, Y. Yang, A. Kozinda, L. Lin, Nano Lett. 13 (2013) 3524e3530.

[11] R. Kumar, H.-J. Kim, S. Park, A. Srivastava, I.-K. Oh, Carbon 79 (2014) 192e202.

[12] G.-H. An, H.-J. Ahn, Carbon 65 (2013) 87e96.

[13] C.H. Kim, B.-H. Kim, J. Power Sources 274 (2015) 512e520.

[14] B.-H. Kim, K.S. Yang, D.J. Yang, Electrochim. Acta 109 (2013) 859e865.

[15] M. Zhi, C. Xiang, J. Li, M. Li, N. Wu, Nanoscale 5 (2013) 72e88.

[16] P. Yang, Y. Chen, X. Yu, P. Qiang, K. Wang, X. Cai, S. Tan, P. Liu, J. Song, W. Mai, Nano Energy 10 (2014) 108e116.

[17] G. Zhang, X.W. Lou, Sci. Rep. 3 (2013) 1470.

[18] X. Yu, B. Lu, Z. Xu, Adv. Mater. 26 (2014) 1044e1051.

[19] L. Peng, X. Peng, B. Liu, C. Wu, Y. Xie, G. Yu, Nano Lett. 13 (2013) 2151e2157.

[20] Y. Liu, Z. Zeng, J. Wei, Front. Nanosci. Nanotechnol. 2 (2016) 78e85.

[21] Z.-M. Huang, Y.Z. Zhang, M. Kotaki, S. Ramakrishna, Compos. Sci. Technol. 63 (2003) 2223e2253.

[22] L. Zhang, A. Aboagye, A. Kelkar, C. Lai, H. Fong, J. Mater. Sci. 49 (2014) 463e480.

[23] K. T~onurist, A. J€anes, T. Thomberg, H. Kurig, E. Lust, J. Electrochem. Soc. 156 (2009) A334eA342.

[24] K. T~onurist, T. Thomberg, A. J€anes, I. Kink, E. Lust, Electrochem. Commun. 22 (2012) 77e80.

[25] K. T~onurist, T. Thomberg, A. J€anes, T. Romann, V. Sammelselg, E. Lust, J. Electroanal. Chem. 689 (2013) 8e20.

[26] C. Yang, Z. Jia, Z. Guan, L. Wang, J. Power Sources 189 (2009) 716e720.

[27] S. Janakiraman, A. Surendran, S. Ghosh, S. Anandhan, A. Venimadhav, Solid State Ionics 292 (2016) 130e135.

[28] J. Hao, G. Lei, Z. Li, L. Wu, Q. Xiao, L. Wang, J. Membr. Sci. 428 (2013) 11e16.

[29] M. Yanilmaz, Y. Lu, J. Zhu, X. Zhang, J. Power Sources 313 (2016) 205e212.

[30] K. T~onurist, I. Vaas, T. Thomberg, A. J€anes, H. Kurig, T. Romann, E. Lust, Electrochim. Acta 119 (2014) 72e77.

[31] W. Ye, B. Amar, G. Ruyan, Mater. Res. Express 3 (2016) 036102.

[32] A. Bund, S. Koehler, H.H. Kuehnlein, W. Plieth, Electrochim. Acta 49 (2003) 147e152.

[33] J. Zhu, M. Chen, H. Qu, Z. Luo, S. Wu, H.A. Colorado, S. Wei, Z. Guo, Energy & Environ. Sci. 6 (2013) 194e204.

[34] G. Wang, H. Xu, L. Lu, H. Zhao, J. Energy Chem. 23 (2014) 809e815.

[35] Q. Wu, M. Chen, K. Chen, S. Wang, C. Wang, G. Diao, J. Mater. Sci. 51 (2016) 1572e1580.

[36] M. Toupin, T. Brousse, D. B_elanger, Chem. Mater. 16 (2004) 3184e3190.

[37] Y. Wang, Y. Song, Y. Xia, Chem. Soc. Rev. 45 (2016) 5925e5950.

[38] T. Wang, D. Song, H. Zhao, J. Chen, C. Zhao, L. Chen, W. Chen, J. Zhou, E. Xie, J. Power Sources 274 (2015) 709e717.

[39] D.P. Dubal, D.S. Dhawale, R.R. Salunkhe, C.D. Lokhande, J. Electrochem. Soc. 157 (2010) A812eA817.

[40] X.-F. Pang, B. Deng, Phys. B Condens. Matter 403 (2008) 3571e3577.

[41] L. Mai, H. Li, Y. Zhao, L. Xu, X. Xu, Y. Luo, Z. Zhang, W. Ke, C. Niu, Q. Zhang, Sci. Rep. 3 (2013) 1718.

[42] P. Simon, Y. Gogotsi, Nat. Mater 7 (2008) 845e854.

[43] Y. Liu, T.D. Dolidze, S. Singhal, D.E. Khoshtariya, J. Wei, J. Phys. Chem. C 119 (2015) 14900e14910.

[44] S. Chen, J. Zhu, X. Wu, Q. Han, X. Wang, ACS Nano 4 (2010) 2822e2830.

[45] J. Zang, X. Li, J. Mater. Chem. 21 (2011) 10965e10969.

[46] W. Tian, Q. Gao, W. Qian, ACS Sustain. Chem. Eng. 5 (2017) 1297e1305.

[47] J. Zhu, M. Chen, H. Wei, N. Yerra, N. Haldolaarachchige, Z. Luo, D.P. Young, T.C. Ho, S. Wei, Z. Guo, Nano Energy 6 (2014) 180e192.

[48] R.K. Singh, R. Devivaraprasad, T. Kar, A. Chakraborty, M. Neergat, J. Electrochem. Soc. 162 (2015) F489eF498.

[49] I. Eremin, A.V. Chubukov, Phys. Rev. B 81 (2010) 024511.